

**A peer-reviewed version of this preprint was published in PeerJ on 7 June 2016.**

[View the peer-reviewed version](https://peerj.com/articles/2111) (peerj.com/articles/2111), which is the preferred citable publication unless you specifically need to cite this preprint.

Zanin M. 2016. On causality of extreme events. PeerJ 4:e2111  
<https://doi.org/10.7717/peerj.2111>

## On causality of extreme events

Massimiliano Zanin

Multiple metrics have been developed to detect causality relations between data describing the elements constituting complex systems, all of them considering their evolution through time. Here we propose a metric able to detect causality within static data sets, by analysing how extreme events in one element correspond to the appearance of extreme events in a second one. The metric is able to detect both linear and non-linear causalities; to analyse both cross-sectional and longitudinal data sets; and to discriminate between real causalities and correlations caused by confounding factors. We validate the metric through synthetic data, dynamical and chaotic systems, and data representing the human brain activity in a cognitive task.

## On causality of extreme events

Massimiliano Zanin<sup>1,2</sup>

<sup>1</sup>*Innaxis Foundation & Research Institute,*

*José Ortega y Gasset 20, 28006, Madrid, Spain*

<sup>2</sup>*Departamento de Engenharia Electrotécnica, Faculdade de Ciências e Tecnologia,*

*Universidade Nova de Lisboa, Lisboa, Portugal*

Multiple metrics have been developed to detect causality relations between data describing the elements constituting complex systems, all of them considering their evolution through time. Here we propose a metric able to detect causality within static data sets, by analysing how extreme events in one element correspond to the appearance of extreme events in a second one. The metric is able to detect both linear and non-linear causalities; to analyse both cross-sectional and longitudinal data sets; and to discriminate between real causalities and correlations caused by confounding factors. We validate the metric through synthetic data, dynamical and chaotic systems, and data representing the human brain activity in a cognitive task.

PACS: 05.45.Tp, 05.45.-a, 87.10.Vg

## I. INTRODUCTION

1  
2 Detecting causality relationships between the elements composing a (complex) system is  
3 an old, though unsolved problem [1, 2]. The origin of the concept of *causality* goes back to  
4 the ancient Greek philosophy, according to which causal investigation was the search for an  
5 answer to the question “why?” [3, 4]; but the debate was still hot in the late 18th century, in  
6 the work of David Hume [5]. Moving to the scientific research, in the last few decades there  
7 has been an increasing interest for detecting causality in real data, which has resulted in the  
8 creation of multiple metrics: Granger causality, cointegration, or transfer entropy [6–10], to  
9 name a few.

10 All proposed metrics share a common characteristic: causality is defined as a relation  
11 existing in the temporal domain, and the metrics thus involve a time series analysis. This  
12 probably originated in the way the human brain conceives causality, as sequences of related  
13 events close in time [11, 12]. This is an important limitation, especially when studying  
14 systems whose dynamics through time cannot easily be observed. Consider, for instance,  
15 genetic analysis; one single measurement is usually available per subject and gene, precluding  
16 the estimation of gene-gene interactions through a causal analysis solely based on expression  
17 levels.

18 Although correlation appears *prima facie* as an interesting solution, it presents the im-  
19 portant drawback of not being able of discriminating between real and spurious causalities.  
20 Suppose one is studying a system composed of three interconnected elements, as the one  
21 depicted in Fig. 1 Left, with the aim of detecting if the dynamics of element  $\mathcal{C}$  is *caused* by  
22  $\mathcal{B}$ ; additionally, no time series are available, and elements are described through vectors of  
23 cross-sectional observations. A statistically significant correlation between  $\mathcal{B}$  and  $\mathcal{C}$  may be  
24 found both when a true causality is present (Fig. 1 Right Bottom), and when both elements  
25 are driven by an unobserved (confounding) element  $\mathcal{A}$  (Fig. 1 Right Top).

26 In order to tackle the scenario of Fig. 1, in this contribution we propose a novel metric  
27 for detecting causality from observational data. It entails three innovative points. First,  
28 it is defined on vectors of observation, which do not have to necessarily represent a time  
29 evolution. In other words, input vectors may correspond to gene expression levels measured  
30 in a population (a cross-sectional study), or (but not necessarily) to multiple observations  
31 of the same subject (a longitudinal study). Second, the method is based on the detection

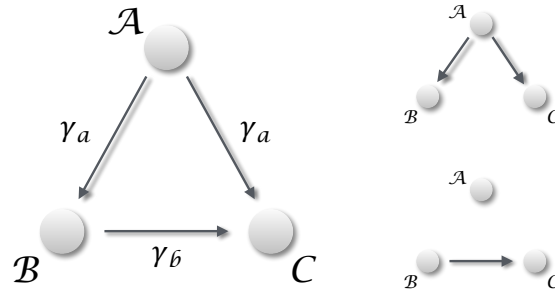


FIG. 1. Distinguishing causality from correlation. (Left) General situation, in which three elements ( $\mathcal{A}$ ,  $\mathcal{B}$  and  $\mathcal{C}$ ) interact in a simple triangular configuration. If one is interested in the relation between  $\mathcal{B}$  and  $\mathcal{C}$ , two different scenarios may arise. (Right top) When  $\mathcal{A}$  is dominating the dynamics, any common dynamics between  $\mathcal{B}$  and  $\mathcal{C}$  will be a correlation, generated by the external confounding factor. (Right bottom) The situation corresponding to a real causality between  $\mathcal{B}$  and  $\mathcal{C}$ .

32 of extreme events, and on their appearance statistics. This is not dissimilar to Granger  
 33 causality, as the latter measures how shocks in one time series are explained by a second  
 34 one; but without the need of a time evolution. Third, it is optimised for the detection of  
 35 non-linear causal relations, which are common in many real-world complex systems [13], but  
 36 that may create problems in standard causality metrics [14].

37

## II. METRIC DEFINITION

38 Suppose two vectors of elements  $\mathcal{B} = \{b_i\}$  and  $\mathcal{C} = \{c_i\}$  of equal size. The two elements  
 39 of each pair  $(b_i, c_i)$  must be related, *e.g.* they may correspond to the measurement of two  
 40 biomarkers in a same subject. In the case of  $\mathcal{B}$  and  $\mathcal{C}$  being time series, clearly  $(b_i, c_i)$  would  
 41 correspond to measurements at time  $i$ ; yet, as already introduced, such dynamical approach  
 42 is not required.

43 Starting from these vectors, some of their elements are labelled as *extreme* when they  
 44 exceed a threshold, *i.e.*  $b_i > \tau_b$  and  $c_i > \tau_c$ . If a causality relation is present between  
 45 them, such that  $\mathcal{B} \rightarrow \mathcal{C}$ , this should affect the way extreme events appear. First, under  
 46 non-extreme dynamics, the two systems  $\mathcal{B}$  and  $\mathcal{C}$  are loosely coupled. Especially when the  
 47 relation is of a non-linear nature, small values in the former system are dampened during  
 48 the transmission. Second, most (ideally, all) of the extreme values of  $\mathcal{B}$  should correspond

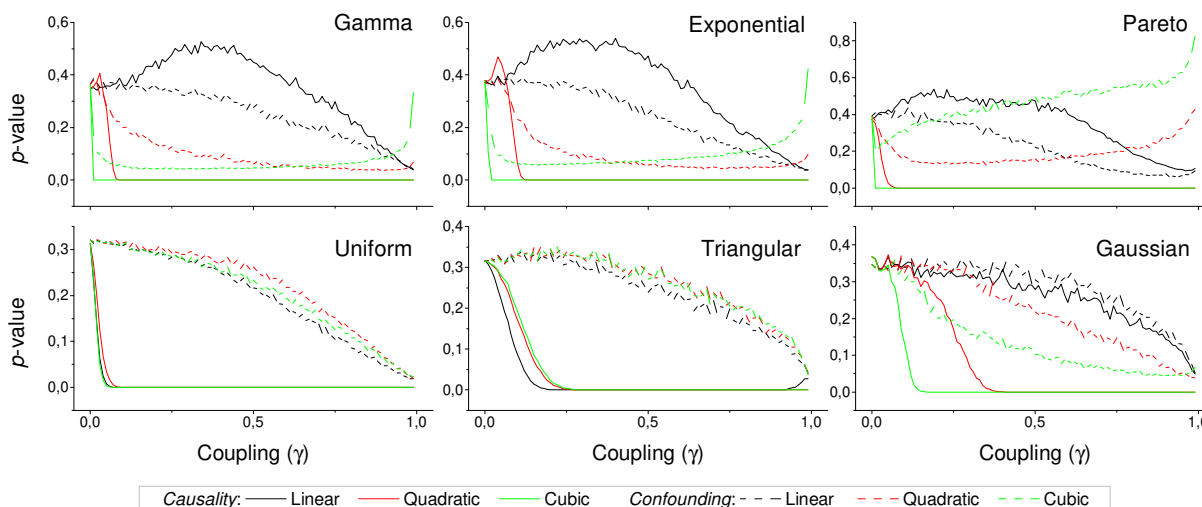


FIG. 2.  $p$ -value obtained by the proposed causality metric, for vectors of synthetic data drawn from six different distributions, as a function of the coupling constant  $\gamma$  - see main text for details. Black, red and green lines respectively correspond to linear, quadratic and cubic couplings; solid lines depict true causalities (as in Fig. 1 Right Bottom), dashed lines spurious ones (Fig. 1 Right Top). Each point corresponds to 10.000 realisations.

49 to extreme values of  $\mathcal{C}$ , as extreme signals will be amplified from the former to the latter  
 50 by the non-linear coupling. Third, extreme values of  $\mathcal{C}$  only partially correspond to extreme  
 51 values of  $\mathcal{B}$ ; due to its internal dynamics,  $\mathcal{C}$  can display extreme events not triggered by the  
 52 other element.

53 Let us denote by  $p_1$  the probability that an extreme event in  $\mathcal{C}$  also corresponds to an  
 54 extreme event in  $\mathcal{B}$ , *i.e.*  $p_1 = P(b_i > \tau_b | c_i > \tau_c)$ . Conversely,  $p_2$  will denote the probability  
 55 that an extreme event in  $\mathcal{B}$  corresponds to an extreme event in  $\mathcal{C}$ , *i.e.*  $p_2 = P(c_i > \tau_c | b_i > \tau_b)$ .  
 56 In the case of a real causality, the second condition implies that  $p_1 \approx 1$ , the third one that  
 57  $p_2 \ll 1$ . On the other hand, in the case of an external confounding effect, and if the two  
 58 thresholds are chosen such that the probability of finding extreme events is the same for  
 59 both elements, it is easy to see that  $p_1 \approx p_2$ . Notice that the same is true if  $\mathcal{B}$  and  $\mathcal{C}$  are  
 60 bidirectionally interacting.

61 The previous analysis suggests that the necessary condition for having a  $\mathcal{B} \rightarrow \mathcal{C}$  causality  
 62 is  $p_1 > p_2$ . The statistical significance can be quantified through a binomial two-proportion  
 63 z-test:

$$z = \frac{p_1 - p_2}{\sqrt{\hat{p}(1 - \hat{p})\left(\frac{1}{n_1} + \frac{1}{n_2}\right)}}, \quad (1)$$

64 with  $n_1$  and  $n_2$  the number of events associated to  $p_1$  and  $p_2$ , and  $\hat{p} = (n_1 p_1 + n_2 p_2) / (n_1 +$   
65  $n_2)$ . The corresponding  $p$ -value can be obtained through a Gaussian cumulative distribution  
66 function.

67 Before demonstrating the effectiveness of the proposed causality metric, it is worth dis-  
68 cussing several aspects of the same.

69 First of all, the attentive reader will notice the similarity of this method with some metrics  
70 for assessing synchronisation in time series. For instance, local maxima and their statistics  
71 were considered in Ref. [15], and event coincidences in Ref. [16]. In both cases, an essential  
72 ingredient is the time evolution: extreme events in one time series are identified and related  
73 to those appearing in a second time series, and the delay required for their transmission  
74 assessed through a time shift optimisation. While this yields an estimation of the direction  
75 of the information flow between two time series, it cannot be applied to systems whose  
76 time evolutions are not accessible. The metric here proposed has the advantage that can be  
77 applied to static data sets, in principle paving the way to the construction of data mining  
78 algorithms based on causality.

79 Second, the metric definition requires setting two thresholds, *i.e.*  $\tau_b$  and  $\tau_c$ . This can  
80 be done using *a priori* information, *e.g.* when a level is accepted as abnormal for a given  
81 biomarker; or by simply explore all the parameters space, in order to assess the values  
82 of  $(\tau_b, \tau_c)$  corresponding to the lowest  $p$ -value. This may result especially useful in those  
83 situations for which the input elements are not well characterised: beyond the identification  
84 of causality relations, this method may also be used to define what an abnormal value is.

85 Third, we have previously stated that the presence of a confounding effect can be correctly  
86 detected, and that in such situations the metric would not detect a statistically significant  
87 causality. According to the Common Cause Principle [1], two variables are unconfounded *iff*  
88 they have no common ancestor in the causal diagram; and ensuring this requires including  
89 the confounding effects in the analysis, *i.e.* detect if there are causalities  $\mathcal{A} \rightarrow \mathcal{B}$  and  
90  $\mathcal{A} \rightarrow \mathcal{C}$  in the diagram of Fig. 1. In the context here analysed, a confounding effect would  
91 be detected as the presence of co-occurring extreme events (generated by the confounding  
92 element) in both vectors of data. This requires the confounding element to influence in the

93 same way both analysed elements, or, in other words, to have the same coupling strength  
94 between  $\mathcal{A} \rightarrow \mathcal{B}$  and  $\mathcal{A} \rightarrow \mathcal{C}$ . Additionally, if the causality  $\mathcal{B} \rightarrow \mathcal{C}$  is mixed with an external  
95 influence, the latter cannot be detected if the strength of the former is greater - that is, a  
96 strong causality can mask a confounding effect. For all this, the proposed method does not  
97 always allow to discriminate true causalities from spurious relationships, although it provides  
98 important clues about which one of these two effects is having the strongest impact.

### 99 III. METRIC EVALUATION

100 We first test the proposed metric with synthetic data. Fig. 2 presents the evolution of  
101 the  $p$ -value for two vectors  $\mathcal{B}$  and  $\mathcal{C}$ , whose values are drawn from different distributions.  
102 Two situations are compared. First, a real  $\mathcal{B} \rightarrow \mathcal{C}$  causality, such that  $c_i = c_i + \gamma b_i^n$  ( $n$   
103 being the order of the coupling) - solid lines in Fig. 2. Second, a confounding effect in which  
104  $b_i = b_i + \gamma a_i^n$  and  $c_i = c_i + \gamma a_i^n$  - dashed lines in Fig. 2. It can be appreciated that the  $p$ -values  
105 of real causalities drop to zero with small values of coupling constants; and that non-linear  
106 couplings perform better than linear ones. In some cases, a confounding effect (especially  
107 when highly non-linear) can foul the metric and yield a low  $p$ -value - see, for instance, the  
108 cubic confounding coupling for a gamma distribution in Fig. 2. Such situations can easily be  
109 identified by comparing the  $p$ -values for  $\mathcal{B} \rightarrow \mathcal{C}$  and  $\mathcal{C} \rightarrow \mathcal{B}$ : in the case of a true causality,  
110 which is by definition directed, the  $p$ -value should be small only for one of them. An example  
111 of this is depicted in Fig. 3, which shows the evolution of the  $p$ -values for a confounding  
112 effect (top panel) and a causality (bottom panel), for vectors of Gamma distributed values.  
113 Once the limitations and requirements about confounding effects, as defined in the previous  
114 section, are taken into account, discriminating between true and spurious causalities only  
115 requires calculating the two opposite  $p$ -values, and checking whether they are both small.

116 The necessity of detecting extreme events introduces a drawback in the method, *i.e.*  
117 the need of having a large set of input values to reach a stable statistics. This problem is  
118 explored in Fig. 4, which depicts the  $p$ -value obtained as a function of the number of input  
119 values. Depending on the kind of relation to be detected, between 2 and 4 thousand values  
120 are required.

121 One of the advantages of the proposed metric is that it can be applied both to cross-  
122 sectional and longitudinal (*i.e.* time evolving) data. Here we show such flexibility in the



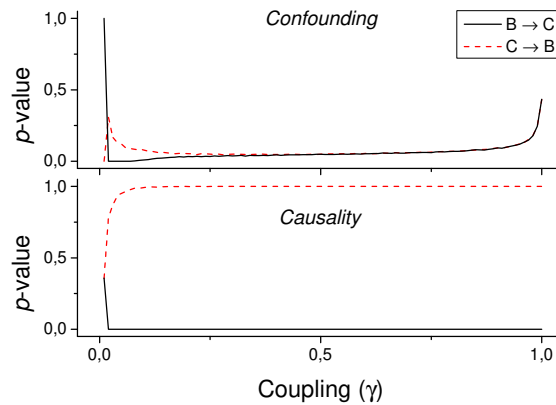


FIG. 3. Evolution of the  $p$ -value of the causality, when considering both  $\mathcal{B} \rightarrow \mathcal{C}$  and  $\mathcal{C} \rightarrow \mathcal{B}$  tests for a cubic coupling and for data drawn from a Gamma distribution (as in green lines of the first panel of Fig. 2). The top panel reports the results for a confounding effect, the bottom one for a true causality between  $\mathcal{B}$  and  $\mathcal{C}$ .

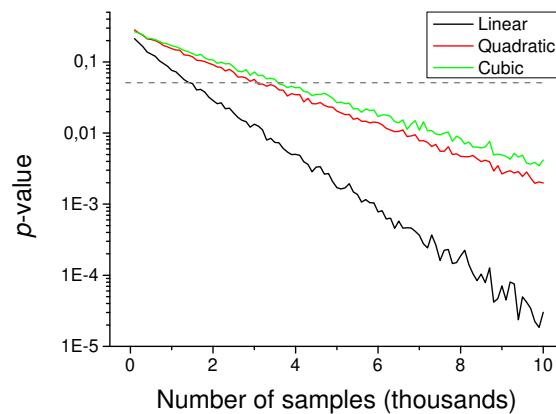


FIG. 4. Evolution of the  $p$ -value of the causality, for a triangular distribution, as a function of the number of values included in the input vectors. Black, red and green lines respectively correspond to linear, quadratic and cubic couplings.

123 detection of the causality between two noisy Kuramoto oscillators [17, 18]. Suppose two  
 124 oscillators whose phases are defined as:

$$\dot{\phi}_{\mathcal{B}} = \kappa_{\mathcal{B}} + \xi \quad (2)$$

$$\dot{\phi}_{\mathcal{C}} = \kappa_{\mathcal{C}} + \gamma \sin(\phi_{\mathcal{B}} - \phi_{\mathcal{C}}) + \xi. \quad (3)$$

125  $\kappa$  is the natural frequency of each oscillator ( $\kappa_{\mathcal{B}} \neq \kappa_{\mathcal{C}}$ ), and  $\xi$  an external uniform noise

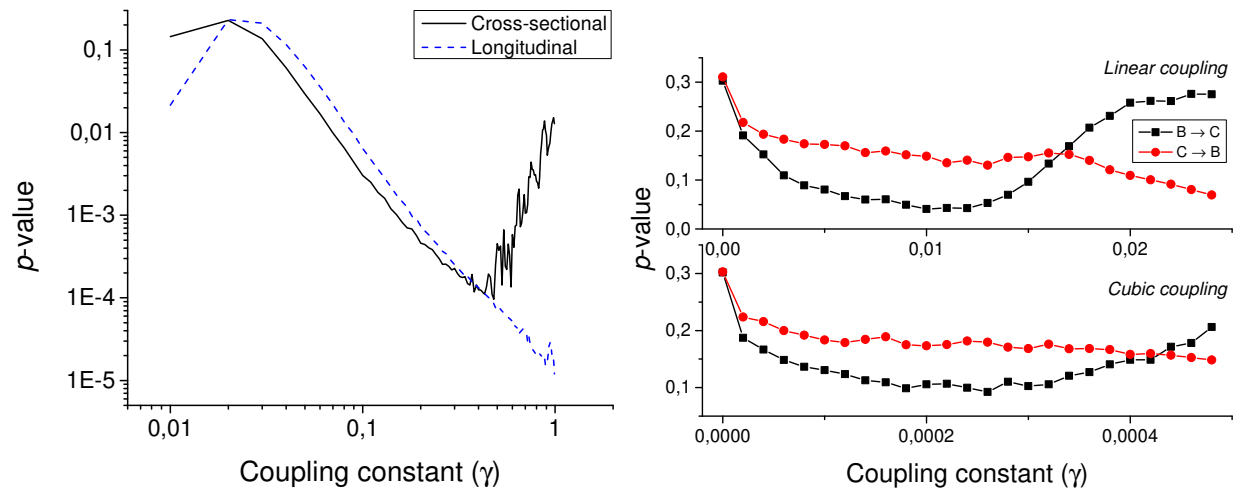


FIG. 5. (Left) Evolution of the  $p$ -value of the causality test between two Kuramoto oscillators, for different values of the coupling constant  $\gamma$ . The solid black line and the dashed blue one respectively correspond to a cross-sectional and longitudinal study - see main text for details. (Right)  $p$ -value for two coupled Rössler oscillators as a function of the coupling constant  $\gamma$ , for a linear (top graph) and cubic (bottom graph) coupling.

126 source. The coupling constant  $\gamma$  defines the way the two oscillators interact, with indepen-  
 127 dent dynamics for  $\gamma \approx 0$ , and a causality  $\phi_B \rightarrow \phi_C$  for  $\gamma > 0$ . The longitudinal causality  
 128 can be detected by considering the time series created by  $\dot{\phi}_B$  and  $\dot{\phi}_C$ , thus focusing on how  
 129 abnormal *jumps* in the phase of the oscillators is transmitted from the former to the latter.  
 130 The  $p$ -value of the metric is represented in Fig. 5 Left by the blue dashed line. The equiva-  
 131 lent cross-sectional analysis requires multiple realisations of the previous dynamics; for each  
 132 one of them, one single pair of values  $(\dot{\phi}_B, \dot{\phi}_C)$  is extracted, corresponding to the largest vari-  
 133 ation of  $\phi_B$  (and thus, to the most extreme jump in the phase of the first oscillator). The  
 134 evolution of the corresponding  $p$ -value is shown in Fig. 5 Left by the black solid line. Both  
 135 the longitudinal and cross-sectional analyses yield similar results, suggesting that dynamical  
 136 and static causalities are equivalent under the proposed metric.

137 An important characteristic of complex systems is that their constituting elements usu-  
 138 ally have a chaotic dynamics [13], making more complicated the task of detecting causality  
 139 between them. We here test the proposed metrics by considering two unidirectionally cou-  
 140 pled Rössler oscillators ( $B \rightarrow C$ ) in their chaotic regime - see [19] for details. We consider  
 141 both linear and cubic couplings; following the notation in [19], this means:

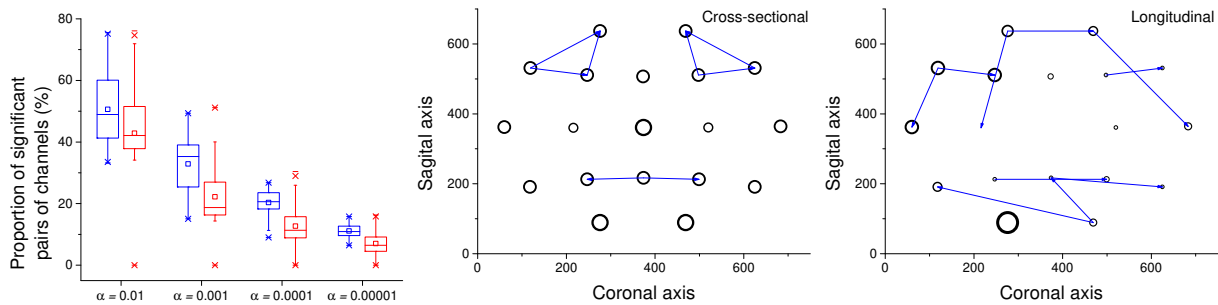


FIG. 6. Analysis of causality in EEG data. (Left) Proportion of pairs of channels in which causality has been detected, for cross-sectional (blue) and longitudinal (red) analyses, as a function of the significance level  $\alpha$ . (Center) Top-10 causality links in the cross-sectional analysis. (Right) Top-10 causality links in the longitudinal analysis. In the central and right panel, the size of the node is proportional to its weight.

$$\dot{y}_1 = -(y_2 + y_3) - \gamma(y_1 - x_1), \text{ and} \quad (4)$$

$$\dot{y}_1 = -(y_2 + y_3) - \gamma(y_1 - x_1)^3. \quad (5)$$

142 Time series are created by sampling the second dimension of each oscillator (*i.e.*  $x_2$  and  
 143  $y_2$ ) with a resolution lower than the intrinsic frequency. Fig. 5 Right depicts the evolution  
 144 of the  $p$ -value for low coupling strengths  $\gamma$ , thus ensuring that the system is *generalised*  
 145 *synchronised*. For  $\gamma \approx 0.01$  ( $\gamma \approx 2 \cdot 10^{-4}$  for cubic coupling), a true causality is detected,  
 146 while for  $\gamma > 0.015$  ( $\gamma > 4 \cdot 10^{-4}$ ) the two oscillators start to synchronise.

147 The possibility of combining a cross-sectional analysis of extreme values with a longitudi-  
 148 nal analysis opens new doors towards the understanding of systems for which both aspects  
 149 can be studied at the same time. Here we show how this can be achieved in the analysis of  
 150 functional networks representing the structure of brain activity in healthy subjects [20, 21].  
 151 The data set corresponds to electroencephalographic (EEG) recordings of 40 subjects during  
 152 50 trials of an object recognition task (details can be found in [22] and references within),  
 153 obtained through the UCI KDD archive [23]. For each trial and subject, 19 time series (cor-  
 154 responding to 19 EEG channels in the 10 – 20 configuration) of 256 samples were available.  
 155 The longitudinal analysis was performed by calculating the causality using the raw time  
 156 series. On the other hand, the cross-sectional analysis relies on identifying the propagation  
 157 of extreme events, as in the case of the Kuramoto oscillators. Extreme events are defined

158 as those for which the energy of the signal is maximum in a given time series; the energy is  
159 defined, at each time point, as the deviation with respect to the mean, normalised by the  
160 standard deviation of the signal - *i.e.* as the absolute value of the Z-Score.

161 Fig. 6 (Left) depicts a box plot of the proportion of significant pairs of channels (*i.e.*  
162 pairs of channels for which a causality was detected), in both the cross-sectional (blue)  
163 and longitudinal (red) analyses, for different significance levels  $\alpha$ . In the case of the cross-  
164 sectional analysis, each value corresponds to the results for a single subject. Results are  
165 qualitatively equivalent, with the longitudinal analysis detecting slightly less links than  
166 the cross-sectional one for small values of  $\alpha$ . Fig. 6 Center and Right depict the 10 most  
167 significant links, as detected by both analyses. While not completely equivalent, both graphs  
168 suggest that some areas are identified as active by both methods, *e.g.* the frontal lobe on the  
169 top and the visual and somatosensory integration area in the bottom. Remarkably, these  
170 two regions are expected to be relevant for the task studied, *i.e.* object identification: the  
171 former for higher function planning (react to the image shown), the latter in the processing  
172 of visual inputs.

#### 173 IV. CONCLUSIONS

174 In conclusion, we presented a novel metric able to detect causality relationships both in  
175 static and time-evolving data sets, thus overcoming the limitation of existing metrics that  
176 rely on time series analysis. The proposed metric is designed to detect the propagation  
177 of extreme events, or shocks, and as such is more efficient when non-linear relations are  
178 present; it is further able to discriminate real from spurious causalities, thus enabling the  
179 detection of confounding effects. The effectiveness of the metric has been tested through  
180 synthetic data, data obtained from simple and chaotic dynamical systems (Kuramoto and  
181 Rössler oscillators), and on EEG data representing the activity of the human brain during  
182 an object recognition task.

183 The possibility of detecting causality in static data sets is expected to be of increasing  
184 importance in those research fields in which time dynamics are not available, and that  
185 require ensuring that a causality is not just the result of the presence of a confounding  
186 factor. For instance, one may consider the rising field of biomedical data analysis [24–  
187 26]. The custom solution is to resort to data mining algorithms, which allow to detect and

188 make explicit patterns in the input data, with the final objective of using such patterns in  
189 diagnostic and prognostic models [27]. Nevertheless, data mining (and machine learning in  
190 general) is based on the Bayes theorem, a form of statistics of co-occurrences, and thus on  
191 a generalised concept of correlation. These methods are thus sensitive to the confounding  
192 effects that are frequently in place, as genes and metabolites create an intricate network  
193 of interactions. Resorting to classical causality metrics, like Granger's one, is not possible,  
194 as time series are seldom available - measuring gene expression or metabolite levels is an  
195 expensive and slow process. In spite of this, causality is an essential element to be detected:  
196 if one only focuses on correlations, there is a risk of detecting elements whose manipulation  
197 does not guarantee the expected results on the system [28–30]. We foresee that the proposed  
198 causality metric can be an initial solution to this problem, by providing a causality test that  
199 can be applied to static data, and that could be used as the foundation of a new class of  
200 data mining algorithms.

201 A Python implementation of the proposed causality metric is freely available at [www.mzanin.com/Causality](http://www.mzanin.com/Causality).

- 
- 203 [1] J. Pearl, *Econometric Theory* **19**, 675 (2003).  
204 [2] J. Pearl, *Causality* (Cambridge university press, 2009).  
205 [3] M. G. Evans, *Philosophy and Phenomenological Research* , 466 (1959).  
206 [4] R. J. Hankinson, *Cause and explanation in ancient Greek thought* (Clarendon Press Oxford,  
207 1998).  
208 [5] D. Hume *et al.*, *An enquiry concerning human understanding* (Alex Catalogue, 1965).  
209 [6] C. W. Granger, *Journal of econometrics* **39**, 199 (1988).  
210 [7] C. W. Granger, *Journal of Economic Dynamics and Control* **12**, 551 (1988).  
211 [8] T. Schreiber, *Physical review letters* **85**, 461 (2000).  
212 [9] M. Staniek and K. Lehnertz, *Physical Review Letters* **100**, 158101 (2008).  
213 [10] P. Verdes, *Physical Review E* **72**, 026222 (2005).  
214 [11] A. M. Leslie and S. Keeble, *Cognition* **25**, 265 (1987).  
215 [12] S. C. Tanaka, B. W. Balleine, and J. P. O'Doherty, *The Journal of Neuroscience* **28**, 6750  
216 (2008).

- 217 [13] S. H. Strogatz, *Nonlinear dynamics and chaos: with applications to physics, biology, chemistry,*  
218 *and engineering* (Westview press, 2014).
- 219 [14] C. W. Granger and T. Terasvirta, OUP Catalogue (1993).
- 220 [15] R. Q. Quiroga, T. Kreuz, and P. Grassberger, *Physical review E* **66**, 041904 (2002).
- 221 [16] J. F. Donges, C.-F. Schleussner, J. F. Siegmund, and R. V. Donner, arXiv preprint  
222 arXiv:1508.03534 (2015).
- 223 [17] Y. Kuramoto, “Chemical oscillations, waves, and turbulence,” (2012).
- 224 [18] Rodrigues, Francisco A, Peron, Thomas K DM, Ji, Peng, and Kurths, Jürgen, *Physics Reports*  
225 (2015).
- 226 [19] N. F. Rulkov, M. M. Sushchik, L. S. Tsimring, and H. D. I. Abarbanel, *Physical Review E*  
227 **51**, 980 (1995).
- 228 [20] E. Bullmore and O. Sporns, *Nature Reviews Neuroscience* **10**, 186 (2009).
- 229 [21] M. Rubinov and O. Sporns, *Neuroimage* **52**, 1059 (2010).
- 230 [22] X. L. Zhang, H. Begleiter, B. Porjesz, W. Wang, and A. Litke, *Brain Research Bulletin* **38**,  
231 531 (1995).
- 232 [23] S. D. Bay, D. Kibler, M. J. Pazzani, and P. Smyth, *ACM SIGKDD Explorations Newsletter*  
233 **2**, 81 (2000).
- 234 [24] J. C. Prather, D. F. Lobach, L. K. Goodwin, J. W. Hales, M. L. Hage, and W. E. Hammond, in  
235 *Proceedings of the AMIA annual fall symposium* (American Medical Informatics Association,  
236 1997) p. 101.
- 237 [25] K. J. Cios and G. W. Moore, *Artificial intelligence in medicine* **26**, 1 (2002).
- 238 [26] J. Han, in *BIOKDD* (2002) pp. 1–2.
- 239 [27] V. Vapnik, *The nature of statistical learning theory* (Springer Science & Business Media, 2013).
- 240 [28] E. Salmon, F. Collette, C. Degueldre, C. Lemaire, and G. Franck, *Human brain mapping* **10**,  
241 39 (2000).
- 242 [29] L. R. Cardon and L. J. Palmer, *The Lancet* **361**, 598 (2003).
- 243 [30] V. A. Vakorin, O. A. Krakovska, and A. R. McIntosh, *Journal of neuroscience methods* **184**,  
244 152 (2009).